Silver – Indium – Tin

Vasyl Tomashik, Rainer Schmid-Fetzer, Ludmila Tretyachenko, Jozefien De Keyzer

Introduction

The phase equilibria in the Ag-In-Sn system were determined experimentally by [2002Liu] using differential scanning calorimetry (DSC), energy dispersive X-ray spectroscopy, XRD and metallographic techniques and have been summarized in [2003Ohn]. Isothermal sections between 180-600°C were determined together with a number of vertical sections. A thermodynamic assessment of this system was carried out using experimental thermodynamic property and phase equilibria data using the CALPHAD method [2000Ohn, 2002Liu, 2003Ohn]. It was shown that the present dataset can be applied for the prediction not only of phase equilibria but also other properties, such as non equilibrium solidification, surface tension and viscosity in solder alloys. Specimens used for the experimental study were equilibrated at 180, 250, 400 and 600°C before quenching into iced water [2002Liu].

The Ag-In-Sn system has been studied both experimentally and by thermodynamic modeling by [1998Kor]. Six ternary alloys were melted, annealed at 250°C for 100 h, quenched in water and analyzed by optical microscopy (OM) and SEM/EPMA. The interfacial reactions between Ag and binary In-Sn alloys were investigated by diffusion couple experiments which were carried out at 250°C for either 1000 min or 100 h. DSC experiments were carried out to determine the melting temperature of some of the alloys. Calculated isothermal sections at 250 and 113°C were given.

[2001Sug] used DSC to investigate the melting/solidification behavior of the alloys in the Sn rich corner of the ternary system. It was shown that strong segregation takes place during cooling of some In-containing solder alloys as the In component is rejected from the solid with excess In remaining in the liquid. At high enough In concentrations (>16 mass%) this segregation results in partial melting of the solder at temperatures above 113°C.

Interfacial reactions between Ag substrates and liquid In-49Sn (here and further compositions of alloys and phases are given in mass%, unless otherwise indicated) [2000Hua, 2001Chu] and 8Ag-In20-Sn [2002Chi] solders were studied in the temperature ranges from 200 to 350°C and from 225 to 325°C, respectively, by means of OM, SEM and EPMA. The formation of Ag_2In and $AgIn_2$ compounds was observed by [2000Hua, 2001Chu]. It was shown that the interfacial reaction products were a scallop-shaped Ag_2In phase enveloped in an outer layer of $AgIn_2$ [2001Chu]: both were identified as single crystals using polarized light under an optical microscope. During the aging of the In-49Sn/Ag soldered specimens at various temperatures ranging from 25 to 100°C, the Ag_2In and $AgIn_2$ intermetallic compounds compete for a dominant role [2001Chu]. At temperatures below 75°C, the $AgIn_2$ expands in proportion to the composition of the Ag_2In phase and the dominant reaction is: $Ag_2In + 3In \rightleftharpoons 2AgIn_2$. At aging temperatures above 75°C, another type of solid/solid reaction becomes dominant: $AgIn_2 + 3Ag \rightleftharpoons 2Ag_2In$. According to the data of [2002Chi], the intermetallic phase $Ag_{2+x}(In,Sn)$ appeared at the interface. Its chemical composition changed from 68.6Ag-22.8In-8.6Sn at 225°C to 69.6Ag-18.9In-11.5Sn at 325°C. The composition of the matrix of the as-cast solder alloy deviated from Sn-20In-2.8Ag to Sn-22.6In-1.2Ag due to the precipitation of Ag_2In particles. DSC indicated a eutectic temperature of 187.9°C for this alloy, but according to the data of [1997Lee], the liquidus and solidus temperatures were reported to be 175 and 187°C respectively. Using DSC, XRD and SEM, [2002Yeh] studied an alloy of the same composition which had been homogenized at 95°C for 100 h. The solidus and liquidus temperatures were determined to be 170.8 and 195.5°C, respectively.

[1994Woo] used XRD to establish that the solid solubility in the Ag-In-Sn system extends to alloys containing at least 10 at.% In and 2 at.% Ag. However, In decreases the solidus slightly and widens the melting range of the equivalent Ag-Sn alloy.

There are two potential candidates (Sn-3.5Ag-5In and Sn-2.8Ag-20In) for Pb-free solders in this system [2002Liu]. It was found that the Sn-2.8Ag-20In alloy is composed of the γ (~ 90%), Ag_2In and $AgIn_2$ phases in the solid state, the Sn-3.5Ag-5In alloy is composed of the γ, (Sn) and ζ phases in the temperature

range from 150-200°C and of the (Sn) and the Ag_2In phase below 150°. It should be noted that the formation of the liquid phase caused by segregation under non equilibrium conditions increases the freezing range. In particular, for the Sn-3.5Ag-5In alloy, a very narrow freezing range exists under equilibrium conditions, while a small fraction of liquid phase exists down to 115°C under non equilibrium conditions.
Samples of about 8 at.% (In + Sn) in Ag, covering the range of 1-8 at.% In, were found to be single phase by metallography [1980Iga, 1988Sch]
Measurement of thermodynamic properties was carried out by [1956Kle, 1987Gat, 2002Liu, 2003Zha].

Binary Systems

The binary systems are accepted from recent thermodynamic calculations supported by additional experimental work as follows: Ag-In [2001Mos], Ag-Sn [1999Oht] and In-Sn [1996Lee]. The three phase diagrams are reproduced in [2002Liu] since they form the basis of that work.

Solid Phases

All crystallographic data are listed in Table 1. Ternary phases were not found in this system over the investigated temperature range [1998Kor]; however, the ζ (hcp) phase forms a continuous series of solid solutions from the Ag-Sn side to the Ag-In side [2002Liu].
The mutual solubilities of In in the Ag_3Sn and that of Sn in the Ag_2In phase are very small.

Invariant Equilibria

The ternary invariant equilibria are given in Table 2 and Fig. 1 [2000Ohn, 2002Liu]. All solid state reactions are taken from the vertical sections presented in [2002Liu], supposedly of U type. According to the work of [1998Kor], a ternary eutectic melts in this system at 114°C (this temperature was reported also in the reviews of [2002Kat, 2003Oul]). The calculation gave two different possibilities for this eutectic reaction: $L \rightleftharpoons Ag_2In + \beta + \gamma$ or $L \rightleftharpoons \zeta + \beta + \gamma$, in which ζ would transform to Ag_2In by a solid state reaction at some temperature lower than the eutectic temperature. This latter option is not accepted here. The composition Sn-50In-2.5Ag (mass%) ($Ag_{0.027}In_{0.507}Sn_{0.466}$) was placed close to the ternary eutectic [2003Oul], which is not far from the accepted value in Table 2. A number of typographical errors in the table given by [2002Liu] were corrected. For example, the temperature of 227°C given for U_1 in [2002Liu] is impossible for this transition type reaction since it is higher than 221°C of the related Ag-Sn eutectic, e_2. The correction was made by recalculating all the ternary and binary phase equilibria using the same thermodynamic parameters as [2002Liu], resulting in 217°C for U_1. From this new calculation, the compositions of all other phases involved in the invariant reactions are given in Table 2; they are not given in [2002Liu]. Also confusion over the phases Ag_2In and $AgIn_2$ is corrected. It is noted that in this, otherwise very extensive and useful work on the ternary system, some other typographical errors are misleading concerning the references of the binary systems used: for Ag-Sn [1999Oht] (not 1995Ohtani) and for In-Sn [1996Lee] (not 1994Lee) is correct.

Liquidus Surface

Based on the optimized thermodynamic parameters, the calculated liquidus projection of the Ag-In-Sn system is shown in Fig. 2 [2000Ohn, 2002Liu, 2003Ohn], in which there are five transition type reactions and one eutectic reaction near the In-Sn edge. This diagram has been checked by recalculation as detailed in the previous section.

Isothermal Sections

The calculated isothermal sections are in good agreement with experimental data [2002Liu, 1998Kor]. Four examples of the calculated and optimized isothermal sections at 400, 250, 180 and 113°C are given in Figs. 3-6 [2002Liu]. The isothermal sections at 250°C and 113°C are not given in the paper by [2002Liu]

but are calculated here using the parameters of [2002Liu]. This was done in order to enable a quantitative comparison of the two isothermal sections given at these temperatures by [1998Kor].
The isothermal section at 113°C, Fig. 6, slightly below the ternary eutectic is in qualitative agreement with the diagram given by [1998Kor], and these authors confirm that 113°C is very close to the eutectic temperature. There is, however, some quantitative difference in the phase boundaries between these two different thermodynamic calculations of [2002Liu] and [1998Kor]. At 250°C, Fig. 4, the agreement between these authors is even better.

Temperature – Composition Sections

Very satisfactory agreement between the calculated vertical sections and the experimental data was obtained by [2002Liu]. Some of the temperature-composition sections are shown in Figs. 7a-7g [2000Ohn, 2002Liu]. The effect of alloying indium on the phase equilibria of the Sn-3.66Ag eutectic alloy is shown in Fig. 8 [2003Ohn].
The influence of In on the eutectic temperature in the Ag-Sn system (221°C) was calculated by [2002Liu] and is shown in Fig. 9. It is seen that the addition of In decreases the eutectic temperature, and the eutectic temperature reaches 200°C when the In content is 15 mass%.
The effects of Ag on the liquidus and solidus of the Sn-20In alloy (Fig. 10a) and on the liquidus temperature of the Sn-51.7In eutectic alloy (Fig. 10b) have been studied by [2000Ohn].
It should be noted that many phase fields have wrong designations and some phase boundaries are missing in the vertical sections in [2002Liu]. This was corrected in the diagrams presented in the present evaluation.

Thermodynamics

The enthalpy change associated with the formation of the ternary Ag-In-Sn alloys from the binary Ag-Sn and In-Sn alloys was studied by quasibinary experiments in the Sn rich range [1956Kle] and the enthalpies of mixing in the liquid state were determined in a heat flow calorimeter at 980°C (Fig. 11) [1987Gat]. The enthalpies of mixing of the alloys in the sections $Ag_{0.9}Sn_{0.1}$-$In_{0.2}Sn_{0.8}$ and $Ag_{0.9}Sn_{0.1}$-$In_{0.4}Sn_{0.6}$ were determined at 893°C. The enthalpies of mixing were calculated from the data for the binary systems and found to be in good agreement with the experimental results.
Based on the phase diagrams, the measured activities, the mass action law and the coexistence theory of metallic melts involving compound formation, models for the mass action concentrations for the Ag-In-Sn metallic melts have been formulated by [2003Zha]. The calculated results agree well with experimental values, showing that the models formulated can embody the structural characteristics of the corresponding melts. The calculated activities of Ag, Sn and In at 1150°C are shown in Fig. 12 [2002Liu, 2003Zha].

Notes on Materials Properties and Applications

Ag-In-Sn alloys are among the most promising candidates for lead-free solders due to their mechanical strength and creep resistance [1997Hua, 1997Lee, 1998Kar, 1998Kor, 2002Kat, 2002Liu, 2002Yeh]. Ultimate tensile strength (UTS) and elongation of the Sn-3.5Ag-5In composition were reported in the review of [1997Hua]. The soldering temperature was given to be 190°C for the alloy Sn-2.8Ag-20In [1997Hua]. UTS and elongation of this alloy at a strain rate of 10^{-3} s^{-1} at room temperature were given as 59.3 MPa and 50.2%, respectively [2002Yeh]. UTS decreased but its elongation increased with increasing testing temperature. The activation energy for creep at a constant strain rate of 10^{-4} s^{-1} was estimated to be 71.4 kJ·mol^{-1} at a low testing temperature (< 50°C) and 51.0 kJ·mol^{-1} in the temperature range from 50 to 100°C [2002Yeh].
It was shown by [1998Kar] that In additions of up to 2% slightly decreased the fatigue life of Sn-3.5Ag alloy due to a loss in ductility. The tensile strength of Sn-3.5Ag-In increases but its ductility decreases with increasing In content. Microstructural observation suggests that In atoms are dissolved in βSn. Thus, the increase in the tensile strength through In addition is probably caused by a solid solution hardening mechanism. Furthermore, this alloy also contains coarse plate like precipitates of Ag_3Sn. The loss of ductility in Sn-3.5Ag-In alloy should also be ascribed to the irregularly shaped second phases of Ag_3Sn.

The Sn-3.5Ag-In alloy has a relatively high fatigue resistance and the addition of In to less than 2% practically does not affect the fatigue life of the binary alloy [1998Kar]. The fatigue life of this alloy remains superior to that of a Sn-37Pb eutectic alloy, even after the addition of 5% In.
Rapidly solidified powder of the composition Ag-6.0Sn-3.0In has commercial importance as an electrical contact material [1992Ver]. The melting point of this alloy is 835.6°C. These alloy powders can be prepared by gas atomization. Important physical properties of such powders (electrical conductivity, hardness, density and microstructure) were determined by [1992Ver].
The corrosion behavior of three Ag-In-Sn alloys in an aqueous NaCl (3%) solution has been studied using a standard three electrode cell [2003Oul]. Good corrosion resistance of the alloys (x_{In}/x_{Sn} = 0.12 and x_{In}/x_{Sn} = 0.2 and x_{Ag} = 0.03 and 0.1) was confirmed and it was shown that an increase in Ag addition induces an increase in the corrosion resistance while the In content has little effect.

Miscellaneous

The $AgIn_2$ and Ag_2In intermetallic compounds dominating at different aging temperatures could affect material properties, which should be taken into consideration in the application of In-49Sn/Ag solder joints [2001Chu].
The growth of the $Ag_{2+x}(In,Sn)$ intermetallic compound has been shown to be a diffusion-controlled process and the activation energy of its growth rate was calculated to be 41.6 kJ·mol^{-1} [2002Chi]. The oxidation behavior of the Ag-In-Sn alloys containing 8 at.% (In + Sn) was studied between 600 and 860°C in air and at 700°C in oxygen [1980Iga].
Silver increases both the surface tension and viscosity of the Sn-20In alloy [2000Ohn].
Density and surface tension of the $(Sn\text{-}3.8Ag)_{eut}$ + 10In liquid alloys have been measured using the maximum bubble-pressure and dilatometric methods in the temperature range from 160-917 and 242-930°C, respectively [2002Liu]. It was shown that the addition of In slightly increases the density in comparison with the binary-eutectic Ag-Sn at 250°C, with the opposite tendency at 960°C.
Structure, electrical resistivity, wettability, melting point, internal friction and elastic moduli of the 2.8Ag-25In-72.2Sn (I) and 2.5Ag-20In-77.5Sn (II) rapidly solidified Pb-free solder alloys have been investigated by [2004Elb]. According to XRD data, these alloys contain a tetragonal Sn phase, tetragonal In_3Sn, orthorhombic Ag_3Sn, cubic Ag_9In_4 and a hexagonal $InSn_4$ phase. Youngs modulus, bulk modulus and shear modulus of the I and II alloys are 25.739 and 21.446 GPa, 35.541 and 28.571 GPa, 9.33 and 7.799 GPa, respectively. These alloys have lower melting points (173.11 and 162.01°C for the I and II alloy, respectively), electrical resistivity and higher elastic modulus than commercial Pb-Sn alloys. In addition, these alloys have good wetting behavior [2004Elb].

References

[1956Kle] Kleppa, O.J., "A Calorimetric Investigation of Some Binary and Ternary Liquid Alloys Rich in Tin", *J. Phys. Chem.*, **60**, 842 (1956) (Thermodyn., Experimental, 15)

[1980Iga] Igarashi, T., Shibata, M., Kodama Y., "The Precipitation Behavior of Oxide During Internal Oxidation of Ag-In-Sn Alloys" (in Japanese), *Nippon Kinzoku Gakkai Shi*, **44**(4), 378-386 (1980) (Crys. Structure, Experimental, 30)

[1987Gat] Gather, B., Schroeter, P., Blachnik, R., "The Enthalpies of Mixing in the Liquid State on the Ternary Systems Ag-In-Sn, Ag-Sn-Sb, Ag-In-Sb and In-Pb-Sb", *Z. Metallkd.*, **78**, 280-285 (1987) (Thermodyn., Experimental, 20)

[1988Sch] Schmid-Fetzer, R., "Silver - Indium - Tin", MSIT Ternary Evaluation Program, in *MSIT Workplace*, Effenberg, G. (Ed.), MSI, Materials Science International Services GmbH, Stuttgart; Document ID: 10.14858.1.20, (1988) (Crys. Structure, Phase Diagram, Assessment, 1)

[1992Ver] Verma, A., Anantharaman, T.R., "Internal Oxidation of Rapidly Solidified Silver-Tin-Indium Alloy Powders", *J. Mater. Sci.*, **27**, 5623-5628 (1992) (Experimental, Electr. Prop., Mechan. Prop., Morphology, Phys. Prop., 13)

[1994Woo] Wood, E.P., Nimmo, K.L., "In Search of New Lead-Free Electronic Solders", *J. Electron. Mater.,* **23**(8), 709-713 (1994) (Phase Diagram, Experimental, 9)

[1996Lee] Lee, B.J., Oh, C.S., Shim, J.H., "Thermodynamic Assessments of the Sn-In and Sn-Bi Binary Systems", *J. Electron. Mater.* **25**(6), 983-991 (1996) (Calculation, Phase Diagram, Phase Relations, Thermodyn., #, 50)

[1997Hua] Hua, F., Glazer, J., "Lead-Free Solders for Electronic Assembly", *Des. Reliab. Solders Solder Interconnect., Proc. Symp.*, 65-73 (1997) (Review, 63)

[1997Lee] Lee, N.-C., "Getting Ready for Lead-Free Solders" (in German), *Soldering Surf. Mount. Technol.*, **9**(2), 65-69 (1997) (Mechan. Prop., Review, 0)

[1998Kar] Kariya, Y., Otsuka, M., "Mechanical Fatigue Characteristics of Sn-3.5Ag-X (X = Bi, Cu, Zn and In) Solder Alloys", *J. Electron. Mater.*, **27**(11), 1229-1235 (1998) (Experimental, Mechan. Prop., 14)

[1998Kor] Korhonen, T.-M., Kivilahti, J.K., "Thermodynamics of the Sn-In-Ag Solder System", *J. Electron. Mater.*, **27**(3), 149-158 (1998) (Calculation, Phase Diagram, Thermodyn., #, *, 34)

[1999Oht] Ohtani, H., Miyashita, M., Ishida, K., "Thermodynamic Study of Phase Equilibria in the Sn-Ag-Zn System", *J. Japan. Inst. Metals*, **63**(6), 685-694 (1999) (Calculation, Phase Diagram, Phase Relations, Thermodyn., Experimental, #, 68)

[2000Hua] Huang, Y.T., Chuang, T.H., "Interfacial Reactions between Liquid In-49Sn Solders and Ag Substrates", *Z. Metallkd.*, **91**(12), 1002-1005 (2000) (Kinetics, Phase Relations, Morphology, Experimental, 12)

[2000Ohn] Ohnuma, I., Cui, Y., Liu, X.J., Inohana, Y., Ishihara, S., Ohtani, H., Kainuma, R., Ishida, K., "Phase Equilibria of Sn-In Based Micro-Soldering Alloys", *J. Electron. Mater.*, **29**(10), 1113-1121 (2000) (Calculation, Phase Diagram, Phase Relations, Thermodyn., 27)

[2001Mos] Moser, Z., Gasior, W., Pstrus, J., Zakulski, W., Ohnuma, I., Liu, X.J., Inohana, Y., Ishida, K., "Studies of the Ag-In Phase Diagram and Surface Tension Measurements", *J. Electron. Mater.* **30**(9), 1120-1128 (2001) (Calculation, Phase Diagram, Phase Relations, Thermodyn., Experimental, #, 27)

[2001Chu] Chuang. T.H., Huang, Y.T., Tsao, L.C., "$AgIn_2$/Ag_2In Transformation in an In-49Sn/Ag Soldered Joint under Thermal Aging", *J. Electron. Mater.*, **30**(8), 945-950 (2001)

[2001Sug] Suganuma, K., "Advances in Lead-Free Electronics Soldering", *Curr. Opin. Solid State Mater. Sci.*, **5**, 55-64 (2001) (Review, Mechan. Prop., 75)

[2002Chi] Chiang, M.I., Chuang, T.H., "Interfacial Reaction Between Liquid Sn-20In-2.8Ag Solder and Ag Substrate", *Z. Metallkd.*, **93**(12), 1194-1198 (2002) (Kinetics, Phase Relations, Morphology, Experimental, 15)

[2002Kat] Kattner, U.R., "Phase Diagrams for Lead-Free Solder Alloys", *JOM,* **12**, 45-51 (2002) (Phase Diagram, Review, 47)

[2002Liu] Liu, X.J., Inohana, Y., Takaku, Y., Ohnuma, I., Kainuma, R., Ishida, K., Moser, Z., Gasior, W., Pstrus, J., "Experimental Determination and Thermodynamic Calculation of the Phase Equilidria and Surface Tension in the Sn-Ag-In System", *J. Electron. Mater.*, **31**(11), 1139-1151 (2002) (Experimental, Assessment, Interface Phenomena, Phase Diagram, Phase Relations, Phys. Prop., Thermodyn., #, *, 28)

[2002Yeh] Yeh, M.S., "Evaluation of the Mechanical Properties of a Ternary Sn-20In-2.8Ag Solder", *J. Electron. Mater.,* **31**(9), 953-956 (2002) (Mechan. Prop., Experimental, 9)

[2003Ohn] Ohnuma, I., Miyashita, M., Liu, X.J., Ohtani, H., Ishida, K., "Phase Equilibria and Thermodynamic Properties of Sn-Ag Based Pb-Free Solder Alloys", *IEEE Trans., Electron. Pack. Manuf.*, **26**(1), 84-89 (2003) (Experimental, Assessment, Phase Diagram, Thermodyn., 21)

[2003Oul] Oulfajrite, H., Sabbar, A., Boulghallat, M., Jouaiti, A., Lbibb, R., Zrineh, A., "Electrochemical Behavior of a New Solder Material (Sn-In-Ag)", *Mater. Let.,* **57**, 4368-4371 (2003) (Electrochemistry, Experimental, 13)

[2003Zha] Zhang, J., "Calculating Models of Mass Action Concentration for Metallic Melts Ag-In-Sn", *Calphad*, **27**(1), 9-17 (2003) (Calculation, Thermodyn., 13)
[2004Elb] El-Bediwi, A., El-Bahay, M.M., "Influence of Silver on Structural, Electrical, Mechanical and Soldering Properties of Tin-Indium Based Alloys", *Rad. Eff. Defects Solids*, **159**, 133-140 (2004) (Crys. Structure, Electr. Prop., Experimental, 18)

Table 1: Crystallographic Data of Solid Phases

Phase/ Temperature Range [°C]	Pearson Symbol/ Space Group/ Prototype	Lattice Parameters [pm]	Comments/References
(Ag) < 961.93	*cF*4 *Fm*$\bar{3}$*m* Cu	*a* = 408.57	at 25°C [Mas2], dissolves up to 21 at.% In and up to 11.5 at.% Sn
(In) < 156.634	*tI*2 *I*4/*mmm* In	*a* = 325.3 *c* = 494.7	at 25°C [Mas2], dissolves up to 10 at.% Sn
(γSn)	*tI*2 ? γSn	*a* = 370 *c* = 337	at 25°C, 9.0 GPa [Mas2]
(βSn) 231.9681 - 13	*tI*4 $I4_1/amd$ βSn	*a* = 583.18 *c* = 318.18	at 25°C [Mas2]
(αSn) < 13	*cF*8 *Fd*$\bar{3}$*m* C (diamond)	*a* = 648.92	[Mas2]
β, (Ag-In) 695 - 660	*cP*2 *Pm*$\bar{3}$*m* CsCl		25-30 at.% In [Mas2] Not considered in [2001Mos]
α′, (Ag-In) < 187	*cP** *Pm*$\bar{3}$*m* ?		25 at.% In [Mas2] Not considered in [2001Mos]
ζ,	*hP*2 $P6_3/mmc$ Mg		[1998Kor, Mas2, V-C2]
Ag_7In_3 < 675		*a* = 296.1 ± 0.2 *c* = 477.8 ± 0.4	21-36 at.% In [2001Mos] [V-C2]
Ag_4Sn < 722		*a* = 296.58 *c* = 478.24	10-23 at.% Sn [1999Oht] [V-C2]
Ag_2In < 300	*cP*52 *P*$\bar{4}$3*m* Cu_9Al_4	*a* = 992.2 ± 0.4	32 at.% In [2001Mos] 31-33.5 at.% In [Mas2] [V-C2]
$AgIn_2$ < 166	*tI*12 *I*4/*mcm* $CuAl_2$	*a* = 688.1 ± 0.4 *c* = 562.0 ± 0.4	67 at.% In [2001Mos] 66.7 at.% In [Mas2] [V-C2]

Phase/ Temperature Range [°C]	Pearson Symbol/ Space Group/ Prototype	Lattice Parameters [pm]	Comments/References
ε, Ag_3Sn	*oP*8		25 at.% Sn [1999Oht]
< 477	*Pmmn*		23.7-25 at.% Sn [Mas2]
	βCu_3Ti	a = 596.8 ± 0.9	[V-C2]
		b = 478.02 ± 0.4	
		c = 518.43 ± 0.9	
β, In_3Sn	*tI*2		12.5-44.5 at.% Sn [1996Lee]
< 142	*I*4/*mmm*	a = 346.3	[V-C2]
	In	c = 440.4	
γ, $InSn_4$ or In_2Sn_9	*hP*1		76-97.5 at.% Sn [1996Lee]
< 223	*P6/mmm*	a = 320.8	for In_2Sn_9 at –10°C [V-C2]
	BiIn	c = 299.7	
		a = 321.77 ± 0.01	for $InSn_4$ at 49°C [V-C2]
		c = 299.88 ± 0.01	

Table 2: Invariant Equilibria

Reaction	T [°C]	Type	Phase	Composition (at.%)		
				Ag	In	Sn
L + Ag_3Sn ⇌ (βSn) + ζ	217	U_1	L	4.22	1.95	93.83
			Ag_3Sn	75	-	25
			(βSn)	0.07	0.54	99.39
			ζ	73.31	7.96	18.73
L + (βSn) ⇌ γ + ζ	209	U_2	L	3.64	6.94	89.42
			(βSn)	0.06	2.01	97.93
			γ	-	3.74	96.26
			ζ	70.98	19.35	9.67
L + ζ ⇌ γ + Ag_2In	180	U_3	L	2.69	26.10	71.21
			ζ	67.8	28.56	3.64
			γ	-	12.76	87.24
			Ag_2In	68	32	
ζ + γ ⇌ (βSn) + Ag_2In	~ 139	U_4 (?)	-	-	-	-
L + (In) ⇌ β + $AgIn_2$	135	U_5	L	1.45	84.55	14.0
			(In)	-	88.26	11.74
			β	-	87.93	12.61
			$AgIn_2$	33	67	-
L + $AgIn_2$ ⇌ β + Ag_2In	119	U_6	L	1.1	61.81	37.09
			$AgIn_2$	33	67	
			β	-	64.79	35.21
			Ag_2In	68	32	
L ⇌ β + γ + Ag_2In	114	E	L	0.94	52.97	46.09
			β	-	56.09	43.91
			γ	-	23.35	76.65
			Ag_2In	68	32	-
Ag_2In + β ⇌ γ + $AgIn_2$	~ 104	U_7 (?)	-	-	-	-
γ + Ag_2In ⇌ $AgIn_2$ + (βSn)	~ 23.6	U_8 (?)	-	-	-	-

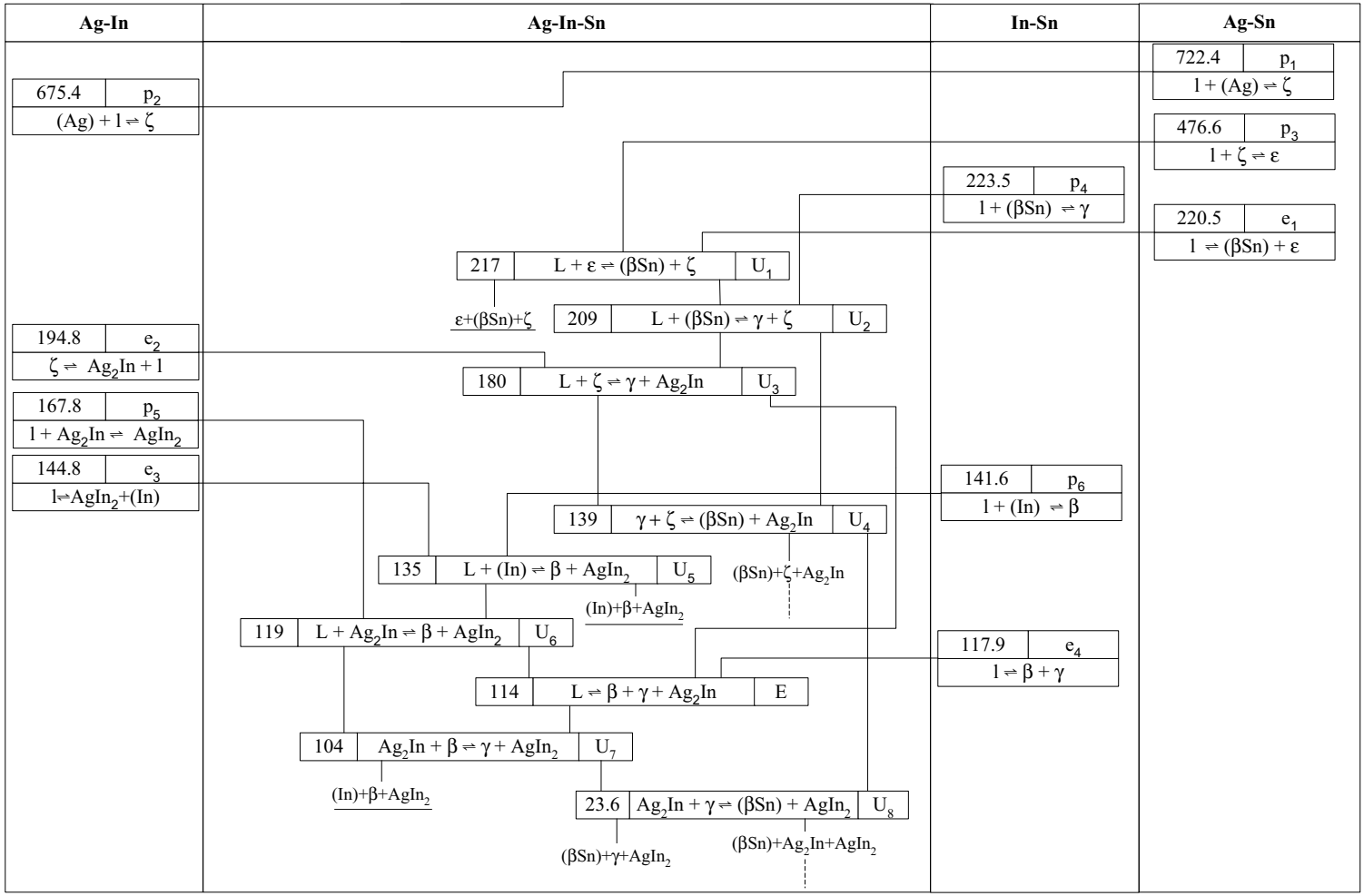

Fig. 1: Ag-In-Sn. Reaction scheme

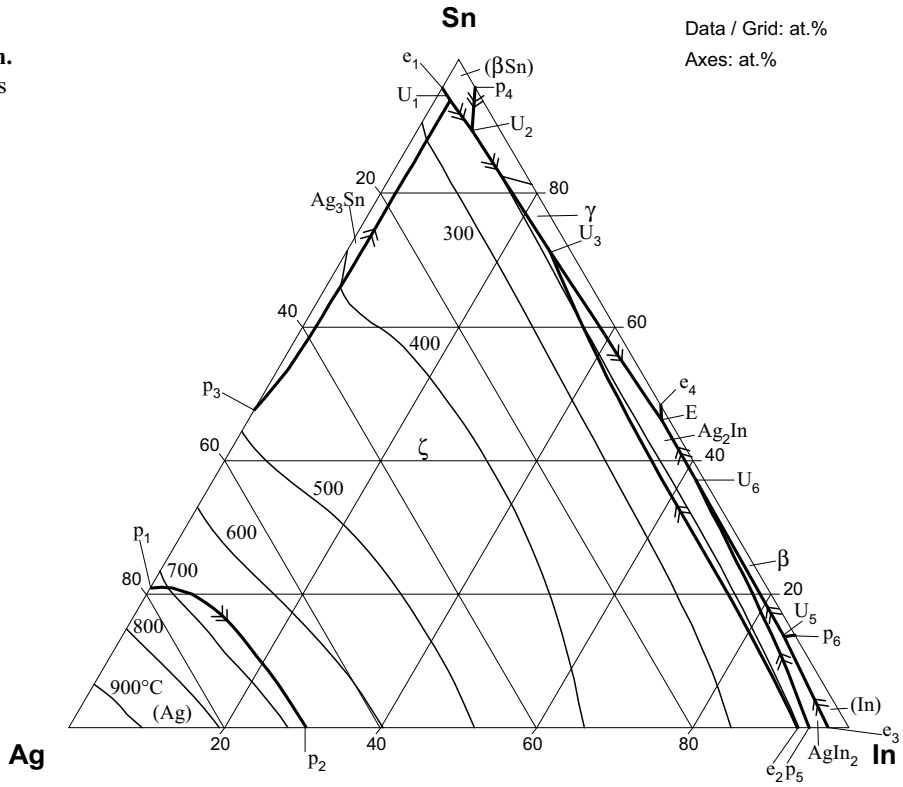

Fig. 2: Ag-In-Sn. Calculated liquidus surface projection

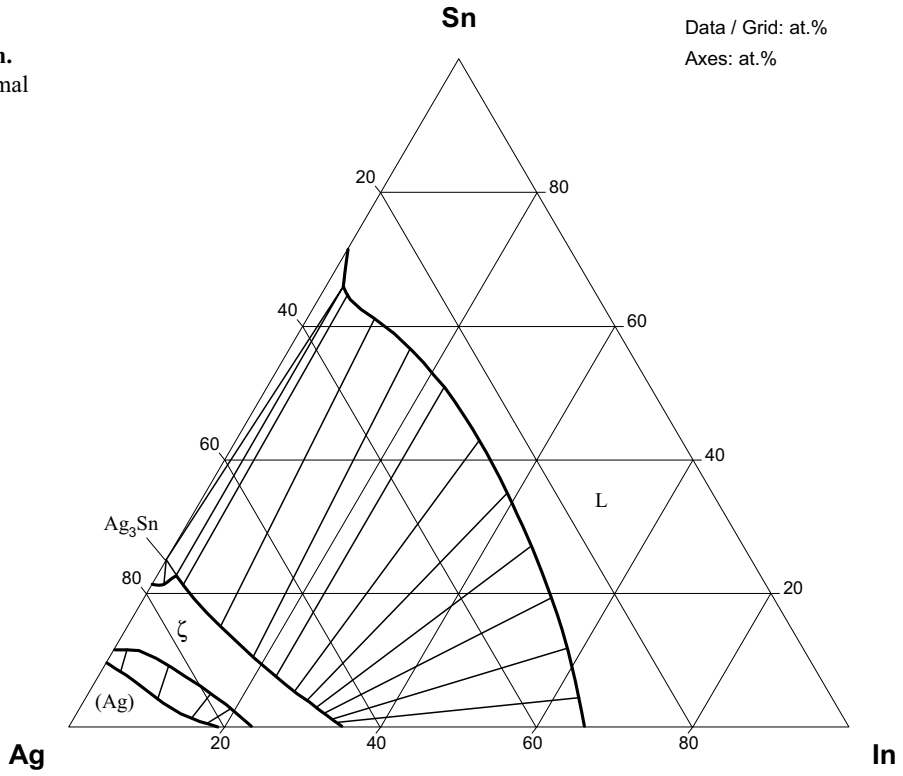

Fig. 3: Ag-In-Sn. Calculated isothermal section at 400°C

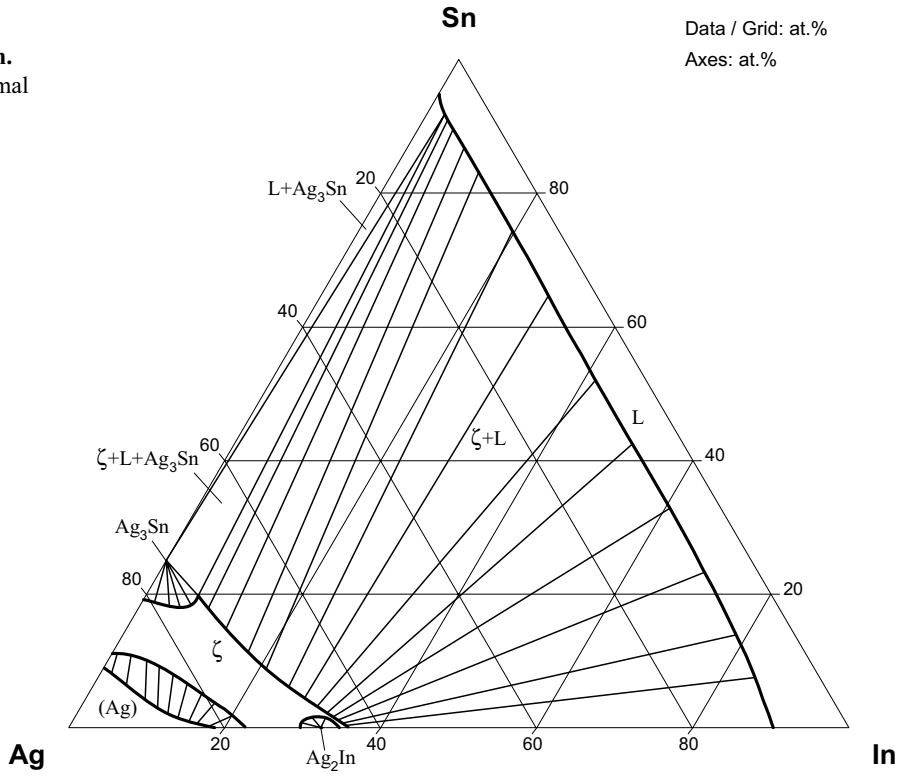

Fig. 4: Ag-In-Sn. Calculated isothermal section at 250°C

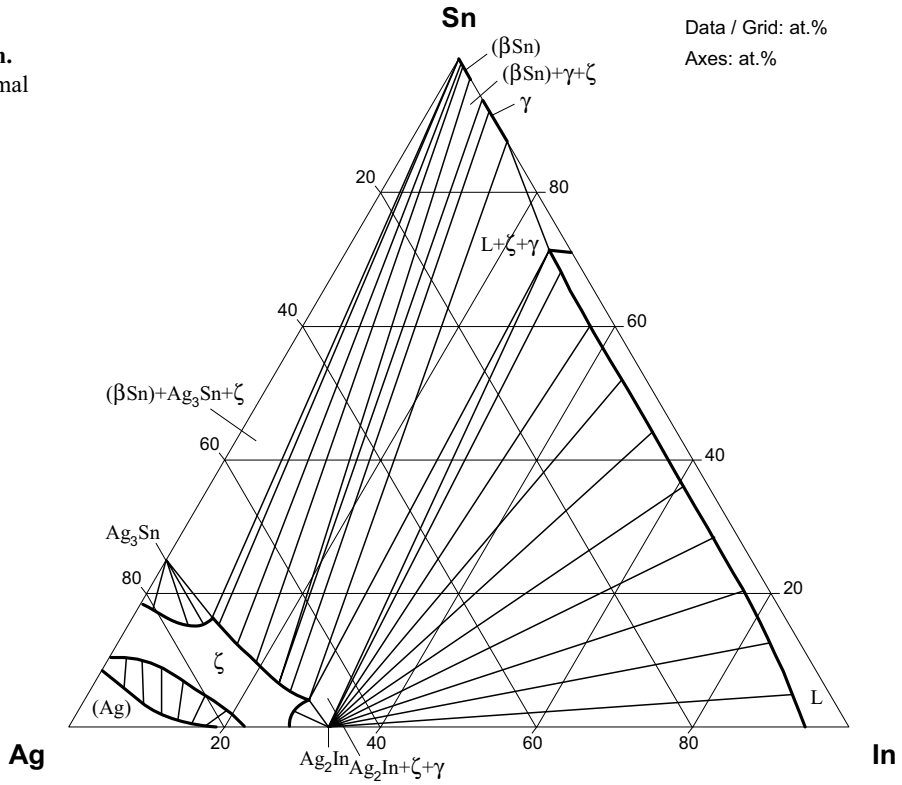

Fig. 5: Ag-In-Sn. Calculated isothermal section at 180°C

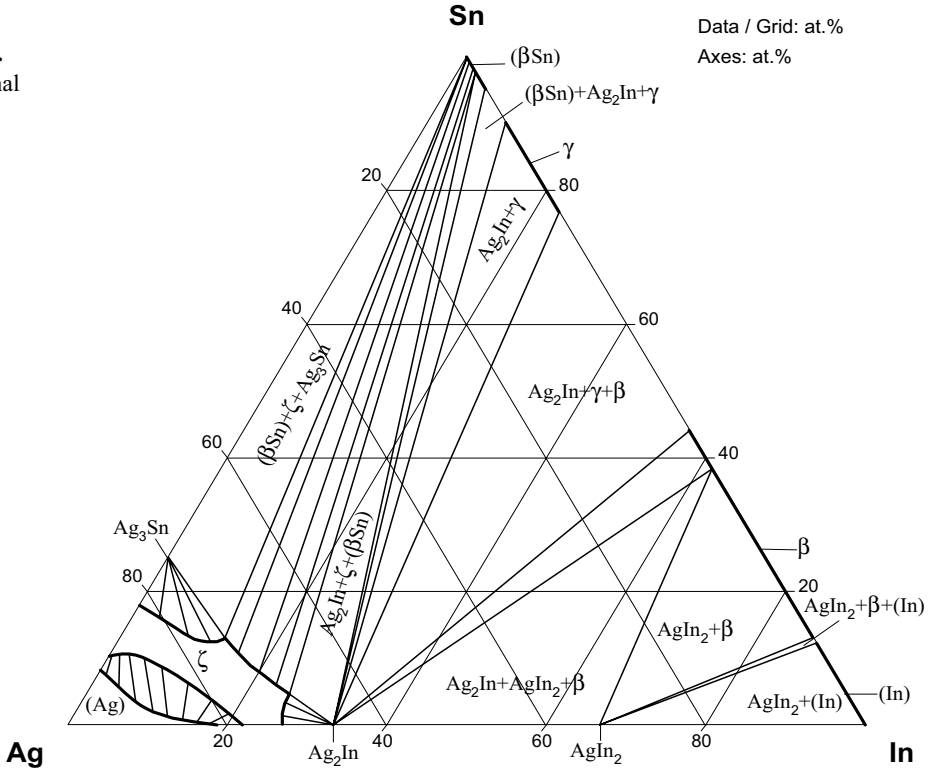

Fig. 6: Ag-In-Sn. Calculated isothermal section at 113 °C

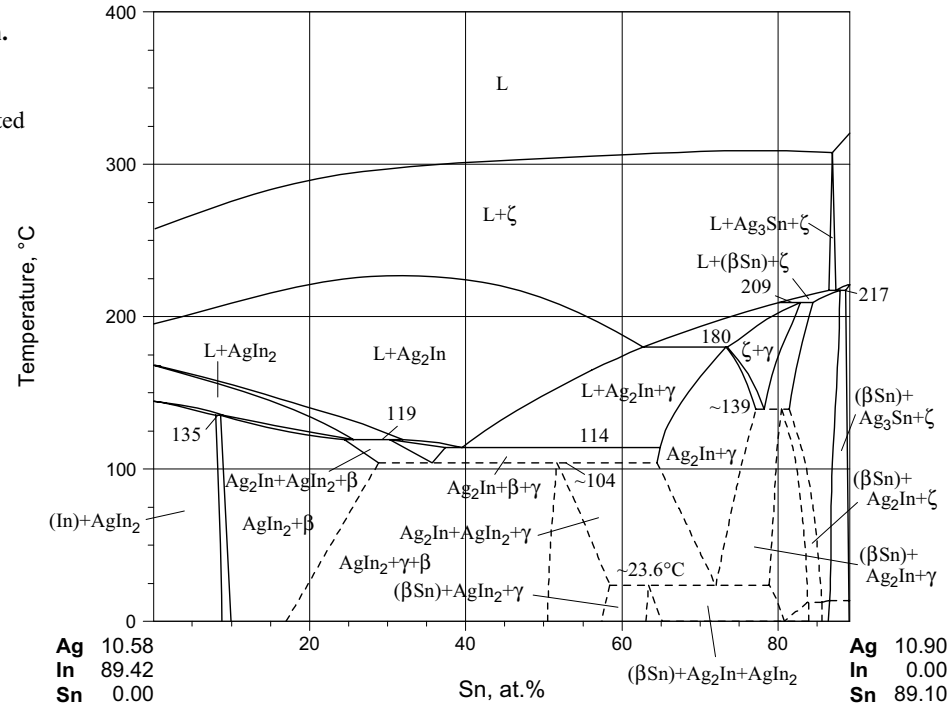

Fig. 7a: Ag-In-Sn. The calculated vertical section at 10 mass% Ag, plotted in at.%

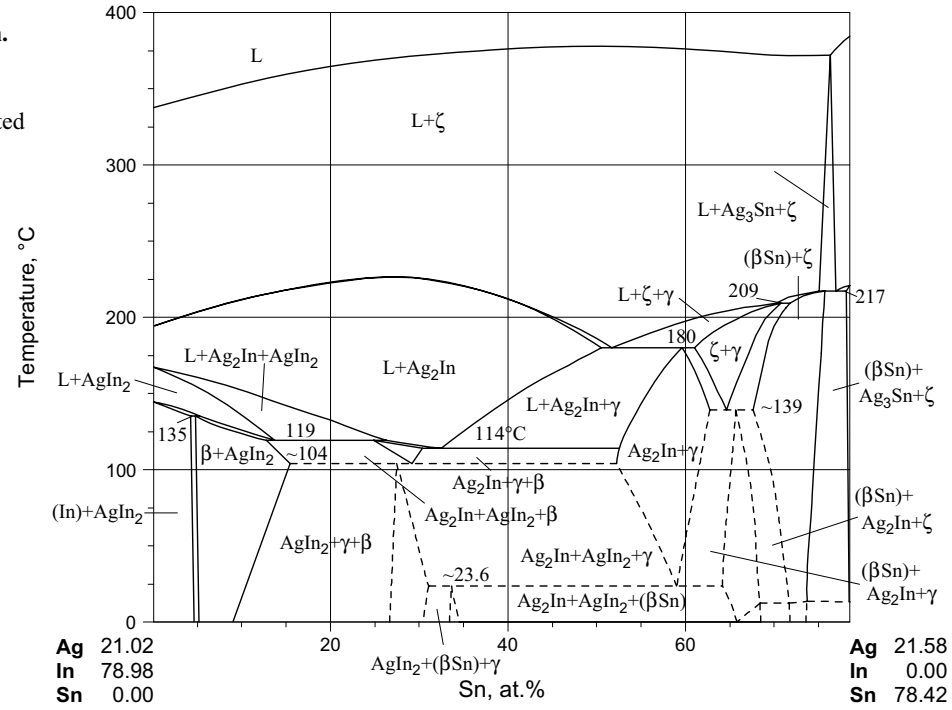

Fig.7b: Ag-In-Sn. The calculated vertical section at 20 mass% Ag, plotted in at.%

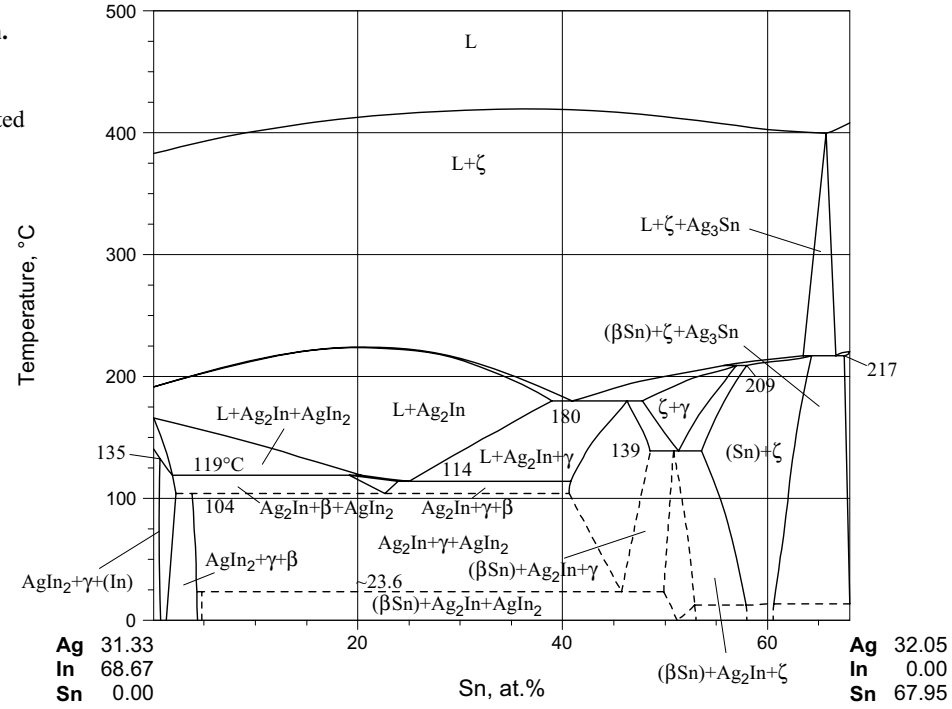

Fig. 7c: Ag-In-Sn. The calculated vertical section at 30 mass% Ag, plotted in at.%

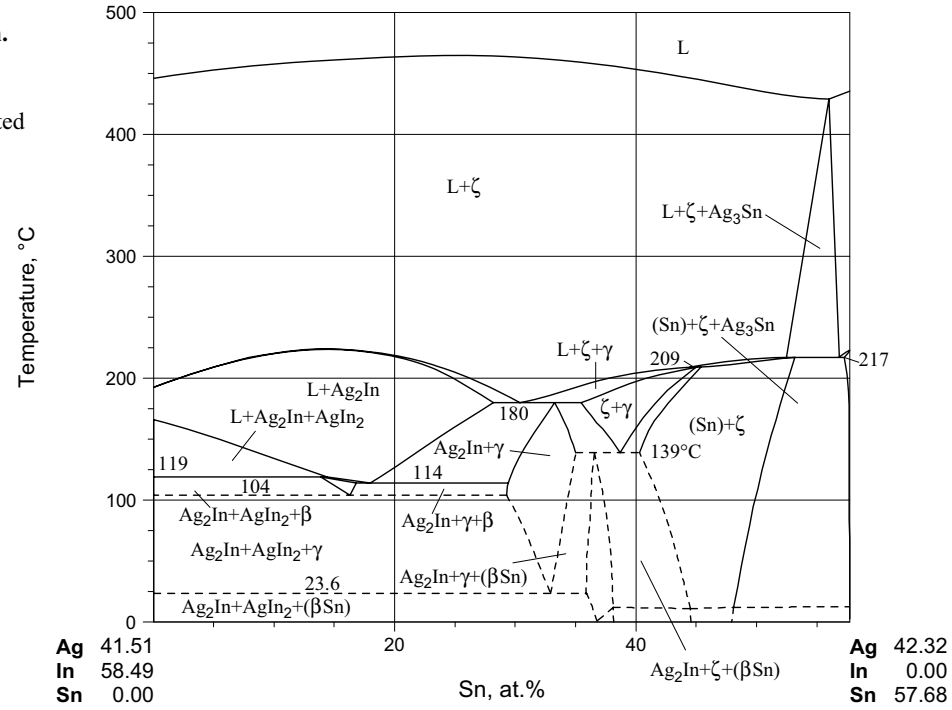

Fig. 7d: Ag-In-Sn. The calculated vertical section at 40 mass% Ag, plotted in at.%

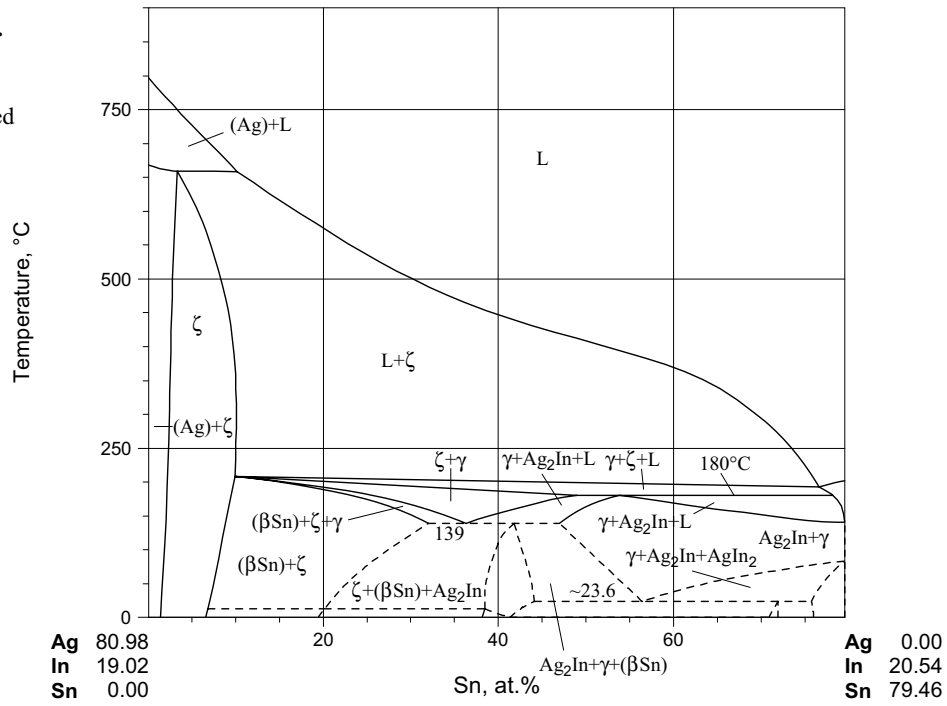

Fig. 7e: Ag-In-Sn. The calculated vertical section at 20 mass% In, plotted in at.%

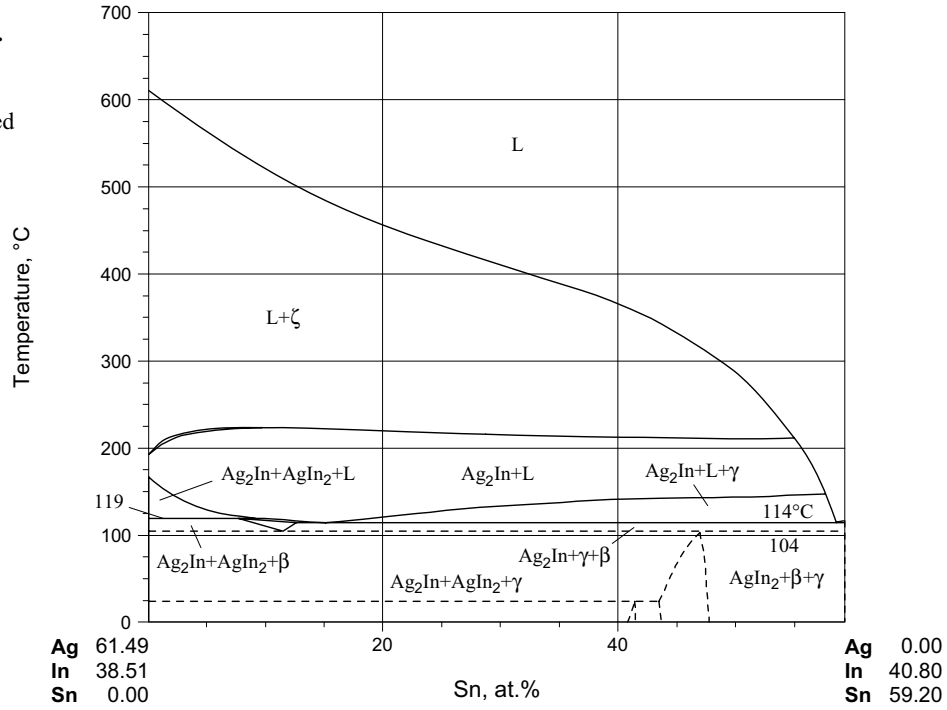

Fig. 7f: Ag-In-Sn. The calculated vertical section at 40 mass% In, plotted in at.%

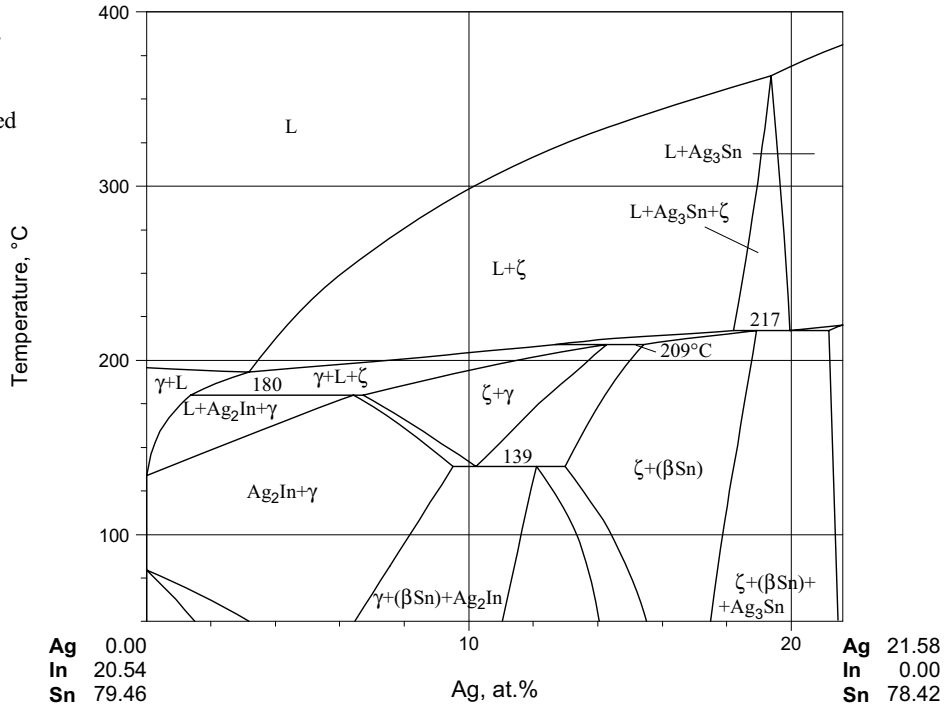

Fig. 7g: Ag-In-Sn. The calculated vertical section at 80 mass% Sn, plotted in at.%

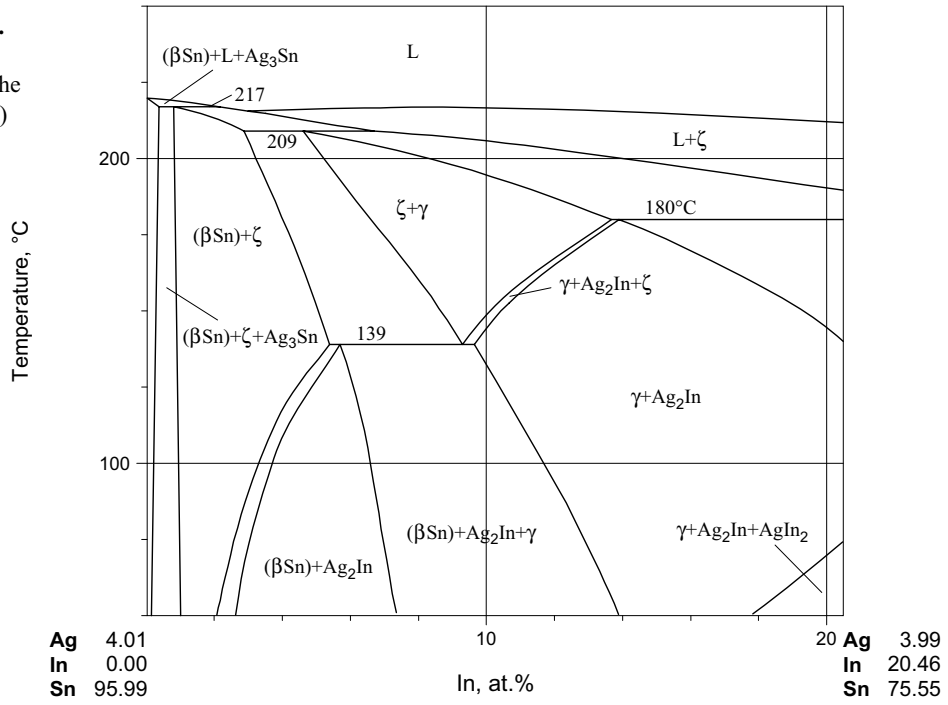

Fig. 8: Ag-In-Sn. Effect of In on the phase equilibria of the Sn-3.66Ag (mass%) eutectic alloys

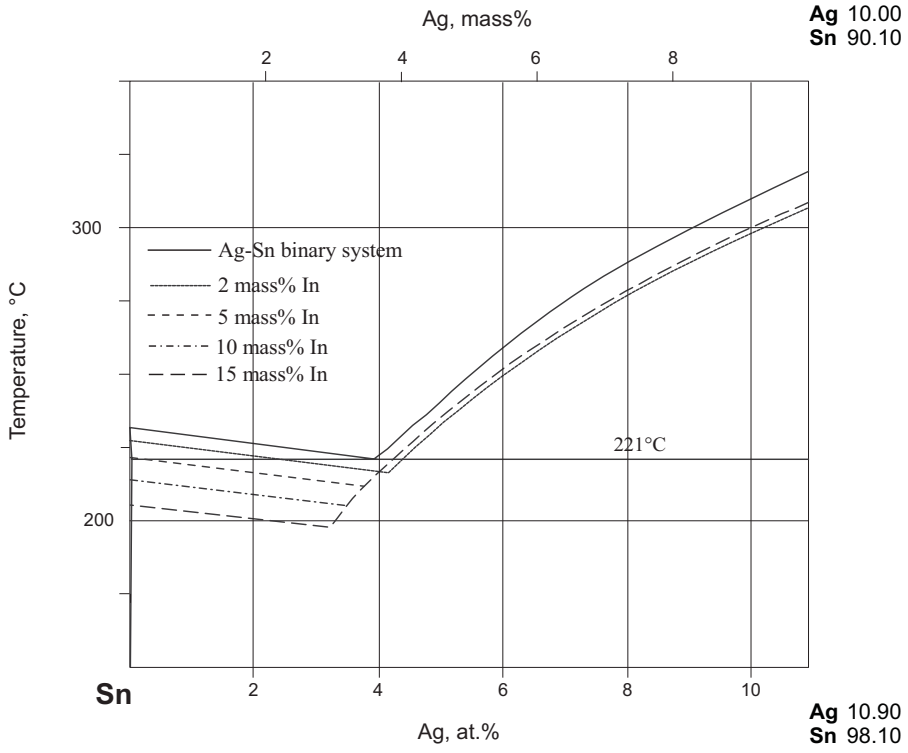

Fig. 9: Ag-In-Sn. Effect of In on the eutectic temperature in Ag-Sn alloys

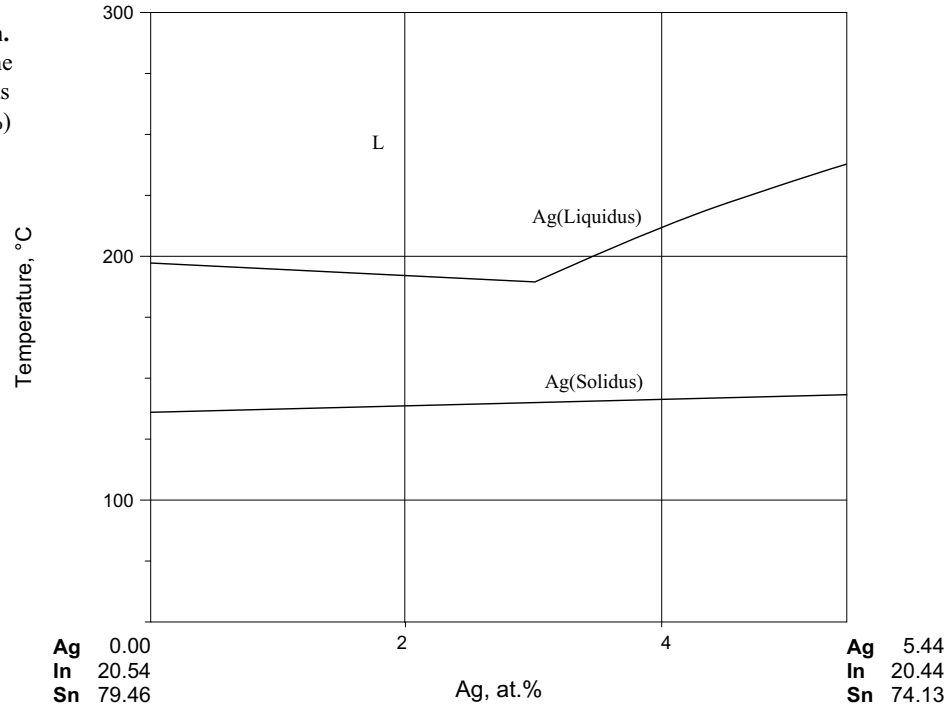

Fig. 10a: Ag-In-Sn. Effects of Ag on the liquidus and solidus of Sn-20In (mass%) alloy

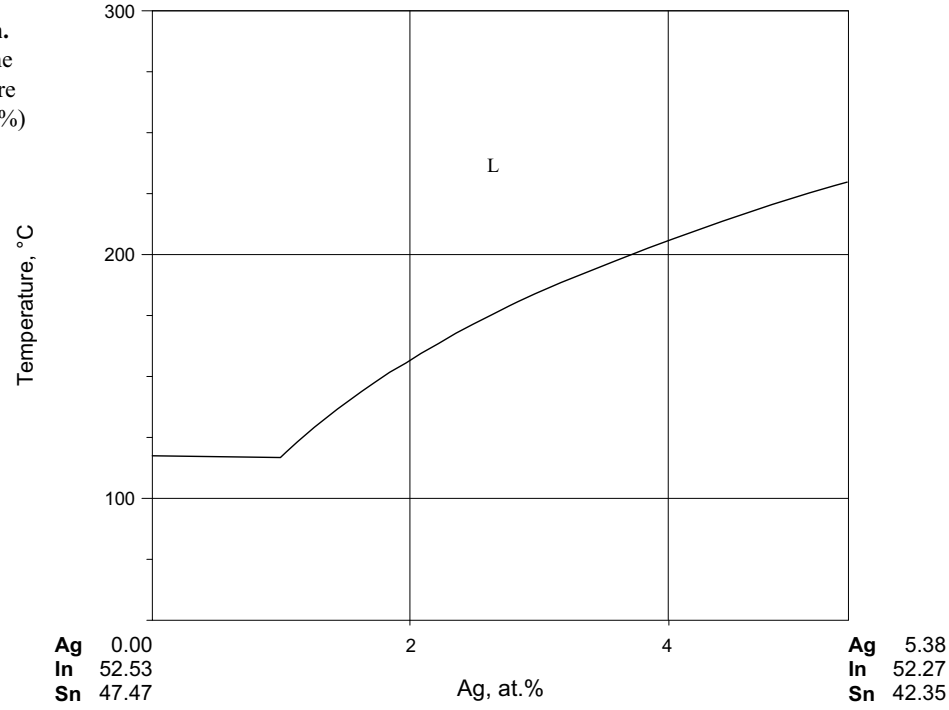

Fig. 10b: Ag-In-Sn. Effects of Ag on the liquidus temperature of Sn-51.7In (mass%) eutectic alloy

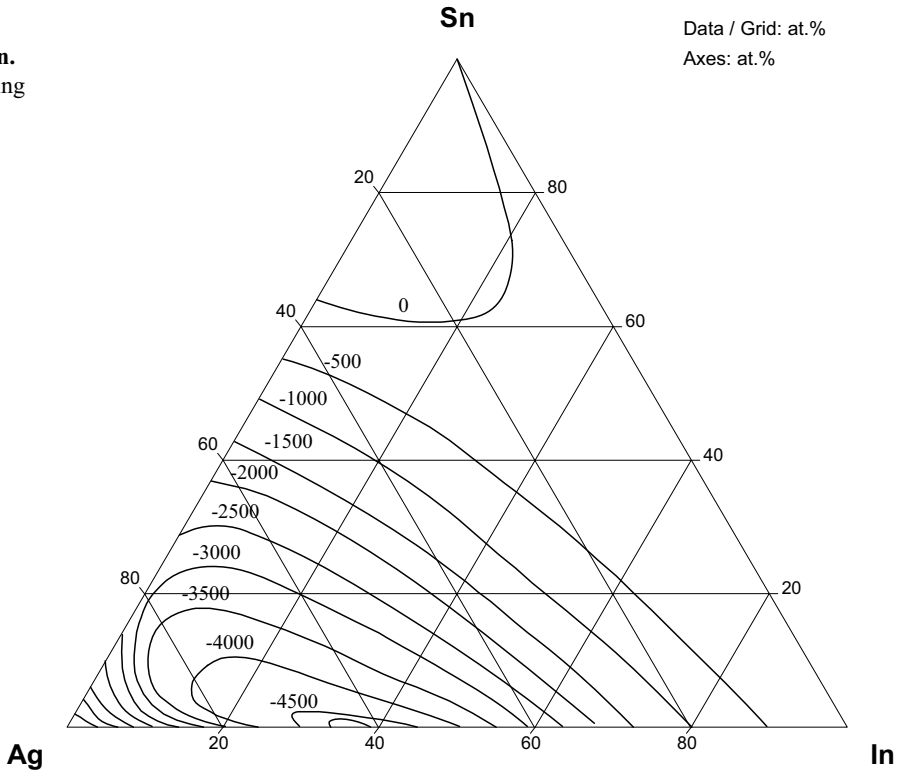

Fig. 11: Ag-In-Sn. Enthalpies of mixing in the liquid state at 980°C

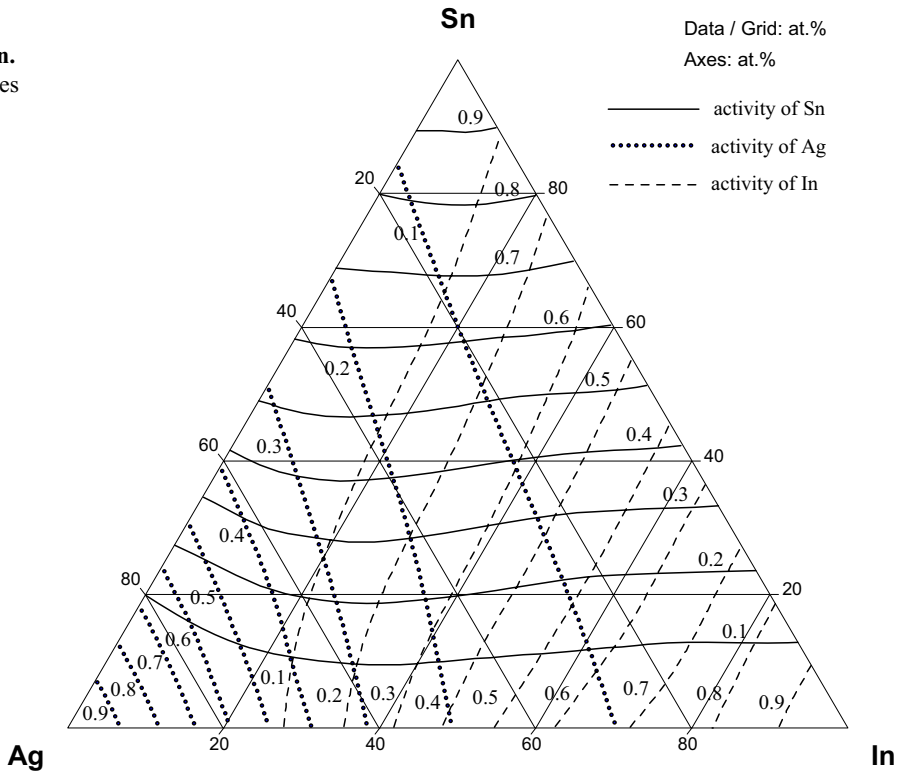

Fig. 12: Ag-In-Sn. Calculated activities of Ag, In and Sn at 1150°C